DMD Fast Forward. Published on April 7, 2010 as DOI: 10.1124/dmd.109.031435
DMD Fast Forward. Published on April 7, 2010 as doi:10.1124/dmd.109.031435

IDENTIFICATION OF THE HUMAN UDP-GLUCURONOSYLTRANSFERASES INVOLVED IN THE GLUCURONIDATION OF COMBRETASTATIN A-4.

Silvio Aprile, Erika Del Grosso, Giorgio Grosa

Dipartimento di Scienze Chimiche, Alimentari, Farmaceutiche e Farmacologiche and Drug and Food Biotechnology Center, Università degli Studi del Piemonte Orientale "A. Avogadro", Largo Donegani 2, 28100 Novara, Italy.

Downloaded from dmd.aspetjournals.org at ASPET Journals on April 9, 2024

Copyright 2010 by the American Society for Pharmacology and Experimental Therapeutics.

DMD Fast Forward. Published on April 7, 2010 as DOI: 10.1124/dmd.109.031435
This article has not been copyedited and formatted. The final version may differ from this version.

RUNNING TITLE PAGE

a) Combretastatin A-4 glucuronidation.

b) Corresponding author:

Silvio Aprile – Dipartimento di Scienze Chimiche, Alimentari, Farmaceutiche e Farmacologiche and Drug and Food Biotechnology Center, Università degli Studi del Piemonte Orientale "A. Avogadro", Largo Donegani 2, 28100 Novara, Italy.

tel +39 (0)321 375855 Fax 39 (0)321 375621

e-mail: silvio.aprile@pharm.unipmn.it

c)

Text pages : 22

Tables : 1

Figures : 4

References: 21

Abstract: 223 words

Introduction: 548 words

Discussion: 921 words

d) Non-standard abbreviations list:

AZT, 3'-azido-3'-deoxythymidine (zidovudine); **CA-4**, (*Z*)-combretastatin A-4; **CA-4G**, (*Z*)-combretastatin A-4 glucuronide; **DAD**; diode array detector; **HLM**, human liver microsomes; **TRIS**, (Tris[hydroxymethyl]aminomethane); **UDPGA** uridine-5'-diphosphoglucuronic acid trisodium salt, **UGTs**, UDP-glucuronosyltransferases.

Downloaded from dmd.aspetjournals.org at ASPET Journals on April 9, 2024

DMD Fast Forward. Published on April 7, 2010 as DOI: 10.1124/dmd.109.031435
This article has not been copyedited and formatted. The final version may differ from this version.

ABSTRACT

The stilbenic compound combretastatin A-4 (**CA-4**) has been described as a potent tubulin polymerization inhibitor. In vivo, **CA-4** binds to tubulin and inhibits microtubule depolymerization, which results in morphological changes in proliferating endothelial cells. Combretastatin A-4 prodrug phosphate is a leading *vascular disrupting agent* (VDA), and is currently being evaluated in multiple clinical trials as a treatment for solid tumors. The aim of this study was to identify and characterize the UGT isoforms involved in **CA-4** glucuronidation by incubation with human liver microsomes and a panel of nine liver expressed recombinant UGT Supersomes™ (1A1, 1A3, 1A4, 1A6, 1A9, 2B4, 2B7, 2B15 and 2B17). As we observed, the high rate of formation of **CA-4G** (V_{max} = 12.78 ± 0.29 nmol/min/mg protein) and the low K_m (6.98 ± 0.65 µM) denoted that UGT1A9 was primarily responsible for the in vitro glucuronidation of **CA-4**. UGT1A6 was also a significant contributor to **CA-4** glucuronidation (V_{max} =3.95± 0.13 nmol/min/mg protein and S_{50} = 44.80 ± 3.54 µM). Furthermore, we demonstrated that the kinetic of **CA-4** glucuronidation with liver microsomes but also with a panel of recombinant UGTs is atypical as it fits two different models: the substrate inhibition and also the sigmoidal kinetic model. Finally, experiments conducted to inhibit the glucuronosyltransferase activity in human liver microsomes assay showed that phenylbutazone, trifluoperazine, propofol and 1-naphtol effectively inhibited **CA-4** glucuronidation.

Downloaded from dmd.aspetjournals.org at ASPET Journals on April 9, 2024

DMD Fast Forward. Published on April 7, 2010 as DOI: 10.1124/dmd.109.031435
This article has not been copyedited and formatted. The final version may differ from this version.

INTRODUCTION

Combretastatin A-4 (**CA-4**) (Fig. 1), a compound isolated from the African bush willow *Combretum caffrum*, has been described as a potent tubulin polymerization inhibitor which also shows cell growth inhibitor properties (Pettit et al., 1989). These features, ultimately, induced the disruption of microtubular function by causing selective and irreversible damage to the neovasculature of tumours (McGown et al., 1989). An increase in vascular permeability is likely to be an important component of the mechanisms that lead to the shutdown of tumour blood flow. Thus **CA-4**, being one of the most important *vascular disruptive agents* (VDAs) is currently in preclinical and clinical development (Tozer et al., 2005). The major problem associated with **CA-4** is its poor solubility in water, hence water soluble combretastatin phosphate prodrug was synthesized (Brown et al., 1995). **CA-4** prodrug phosphate, which was intravenously administered by brief infusion, completed phase I clinical trials and four studies have been published showing that **CA-4** was safe, well-tolerated, and lacking in hematological toxicity. A marked reduction of blood flow in a variety of tumors at doses lower than the MTD was also observed (Banerjee et al., 2008). In these studies it has also been stated (Dowlati et al., 2002; Rustin et al., 2003) that the formation of glucuronide is the main metabolic pathway which contributes to the clearance of **CA-4**. Currently two phase II/III clinical trials are underway for **CA-4**; the first to evaluate the safety and efficacy of **CA-4** in association with paclitaxel and carboplatin in the treatment of anaplastic thyroid cancer (ATC) and the second to determine the safety, tolerability and efficacy of **CA-4** phosphate in combination with bevacizumab, carboplatin and paclitaxel in patients with chemotherapy naïve non-small cell lung cancer (see the web sites: http//:www.cancer.gov and http//:www.oxigene.com). Recently, we elucidated the in vitro/vivo metabolic fate of **CA-4** through identifying the structures of a series of phase I metabolites and the glucuronide conjugate. The formation of sulphate metabolite has also been demonstrated both in vitro and in vivo. (Aprile et al. 2007 and 2009). UDP-glucuronosyltransferases (UGTs) are the major phase II drug metabolism

Downloaded from dmd.aspetjournals.org at ASPET Journals on April 9, 2024

DMD Fast Forward. Published on April 7, 2010 as DOI: 10.1124/dmd.109.031435
This article has not been copyedited and formatted. The final version may differ from this version.

enzymes in humans, catalyzing the conjugation with UDP-glucuronic acid of numerous endogenous and exogenous compounds. Glucuronidation occurs mainly in the liver but also in various extrahepatic tissues, possibly affecting the pharmacokinetics of the administered drugs. Known UGTs are divided into two families: UGT1A and UGT2B. Based on their mRNA levels, it was recently stated that UGT1A1, 1A3, 1A4, 1A6, 1A9, 2B4, 2B7, 2B10, 2B15 and 2B17 are highly expressed in the human liver (Izukawa et al., 2009 and Ohno and Nakajin 2009). To the best of our knowledge, no study reporting the isozymes involved in **CA-4** glucuronidation has been published. The identification of the hepatic UGT isoforms involved in **CA-4** glucuronidation would help to predict the influence of interindividual variation due to polymorphisms on drug bioavailability, pharmacokinetics, and efficacy. Indeed, since it has been demonstrated (Brown et al., 1995) that **CA-4G** is characterized by very low pharmacodynamic activity, a different rate of glucuronidation could affect the **CA-4** therapeutic effect. Moreover, glucuronidation could also modulate the formation of quinone species whose role in **CA-4** pharmacodynamics is at the present time unknown (Aprile et al. 2007). This paper describes the full in vitro kinetic characterization of the hepatic UGT isoforms involved in the **CA-4** glucuronidation pathway.

Downloaded from dmd.aspetjournals.org at ASPET Journals on April 9, 2024

DMD Fast Forward. Published on April 7, 2010 as DOI: 10.1124/dmd.109.031435
This article has not been copyedited and formatted. The final version may differ from this version.

METHODS

Chemicals and Reagents.

Acetonitrile (HPLC grade) was purchased from Sigma-Aldrich (Milano, Italy). Water (HPLC grade) was obtained from ELGA PURELAB *ultra* (M-medical, Milano, Italy). 1-naphthol, alamethicin, AZT, phenylbutazone, propofol, silibinin, trifluoperazine and UDPGA were purchased from Sigma-Aldrich. (Milano, Italy) and used without further purification. **CA-4** and **CA-4G** were prepared according to the procedures cited in the literature. (Aprile et al. 2009).

Combretastatin A-4 glucuronidation assay.

Human Liver Preparations.

The human liver microsomes (HLM) (pooled mixed sex, fifty individual donors, protein concentration: 20 mg/mL, total CYP: 360 pmol/mg protein, rate of formation of estradiol glucuronide (UGT1A1): 1300 pmol/min/mg, trifluoperazine glucuronide (UGT1A4): 730 pmol/min/mg, serotonin glucuronide (UGT1A6): 10,000 pmol/min/mg, propofol glucuronide (UGT1A9): 3300 pmol/min/mg, AZT glucuronide (UGT2B7): pmol/min/mg) were purchased from BD Gentest™ (Woburn, MA). The incubations were all performed using a horizontal DUBNOFF shaking thermostatic bath (Dese Lab Research, Padova, Italy) and were protected from light.

Recombinant UGTs.

Microsomes prepared from baculovirus-infected insect cells which expressed the human UGTs 1A1, 1A3, 1A4, 1A6, 1A9, 2B4, 2B7, 2B15 and 2B17 (Supersomes™; protein concentration: 5 mg/mL) were obtained from BD Gentest™ (Woburn, MA). The glucuronidation activity of Supersomes™ was provided by the supplier for the following substrates: estradiol (UGT 1A1 and 1A3), trifluoperazine (UGT 1A4), 7-hydroxy-4-trifluoromethylcoumarin (UGT 1A6,1A9, 2B4, 2B7 and 2B15) and eugenol (UGT2B17).

Downloaded from dmd.aspetjournals.org at ASPET Journals on April 9, 2024

DMD Fast Forward. Published on April 7, 2010 as DOI: 10.1124/dmd.109.031435
This article has not been copyedited and formatted. The final version may differ from this version.

HLM and recombinant UGT isoform incubation procedures.

Combretastatin A-4 glucuronidation activity was determined both in pooled HLM and in a panel of nine human liver expressed recombinant UGT isoforms. The conditions for linearity with respect to time were optimized at 0.05 mg/mL protein concentration for HLM and UGT1A9 and at 0.5 mg/mL for the other UGTs. The standard incubation mixture, contained in Eppendorf® tubes, was made up of 7.5-500 µM of **CA-4** and 10 mM of $MgCl_2 \cdot 6H_2O$ in a TRIS·HCl buffer (50 mM, pH 7.4) which was brought up to a final volume of 150 µL. The final concentration of acetonitrile in the incubation mixture was 1%. An appropriate volume of HLM or UGT suspension, previously activated by alamethicin (50 µg/mg protein) at 4°C for 15 min, was added to give a final protein concentration of 0.05 mg/mL for HLM or UGT1A9 assays and 0.5 mg/mL for other UGTs. After pre-incubation in a shaking water bath at 37°C the reaction was activated by an appropriate volume of UDPGA solution (2 mM final concentration) and the resulting mixture shaken at 37°C for 9 minutes in HLM, 10 minutes in UGT1A1, 1A3, 1A6, 1A9, 2B17 and 20 minutes in UGT1A4, 2B4, 2B7, 2B15 incubations assays. The reaction was quenched by diluting the samples with 37.5 µL of ice-cold formic acid solution (25% *v/v*). The samples were then centrifuged at 11,000 rpm for 5 min, and the supernatant was directly injected onto the HPLC column for analysis.

Inhibition of HLM, UGT1A9 and UGT 1A6 glucuronidation activity.

Inhibition of combretastatin A-4 glucuronidation was evaluated using known chemical UGT inhibitors. Incubations were performed using HLM (0.1 mg/mL protein concentration) and 100 µM **CA-4** concentration in the same conditions as above, except for the microsomes activation performed using Brij 58 surfactant (0.5 mg/mg protein) in place of alamethicin. Increased concentrations of 1-naphthol (5-500 µM), AZT (50 µM-1 mM), phenylbutazone (5 µM-1 mM), propofol (5 µM-1 mM), silibinin (2.5-100 µM) and trifluoperazine (5-500 µM) were used to inhibit UGT1A6/1A9 (Fujiwara et al., 2008 and Luukkanen et al., 2005), UGT2B7 (Picard et al., 2005), UGT1A (Kerdpin et al., 2008), UGT1A9 (Picard et al., 2005), UGT1A1 (Sridar et al., 2004) and

Downloaded from dmd.aspetjournals.org at ASPET Journals on April 9, 2024

DMD Fast Forward. Published on April 7, 2010 as DOI: 10.1124/dmd.109.031435
This article has not been copyedited and formatted. The final version may differ from this version.

UGT1A4 (Uchaipichat et al., 2006) isoforms respectively. Since trifluoperazine is a known selective substrate for UGT1A4, it was used as the putative inhibitor of the same UGT (Fujiwara et al., 2008). Using the same conditions, the inhibitory effect of 1-naphthol and trifluoperazine was then evaluated on UGT1A9 and UGT1A6 glucuronidation activity. Finally, the inhibitory effect of combretastatin A-4 glucuronide per se on the **CA-4** glucuronidation was studied by adding **CA-4G** to the incubation mixture at a concentration range of 2-12 µM for HLM and 3-6 µM for recombinant UGT1A9 assays.

Kinetic analysis of combretastatin A-4 glucuronidation.

Kinetic constants for HLM and recombinant UGT isoforms were obtained by fitting experimental data to the following kinetic models using Prism 5.0 software (GraphPad Software Inc. San Diego, CA). Data points represent the mean of triplicate experiments.

- *Michaelis-Menten model* (Houston and Kenworthy, 2000);

$$v = \frac{V_{\max} * S}{K_m + S} \qquad (eq.1)$$

where v is the rate of glucuronidation reaction, V_{max} is the maximum reaction rate, K_m is the Michaelis-Menten constant (substrate concentration at ½ V_{max}) and S is the substrate concentration.

- *Substrate inhibition model* (Houston and Kenworthy, 2000);

$$v = \frac{V_{\max} * S}{K_m + S * \left(1 + \frac{S}{K_i}\right)} \qquad (eq.2)$$

where K_i is the substrate inhibition constant.

- *Sigmoidal kinetic model* (Hill equation) (Houston and Kenworthy, 2000);

$$v = \frac{V_{\max} * S^n}{S_{50}{}^n + S^n} \qquad (eq.3)$$

where S_{50} is the substrate concentration resulting in ½ V_{max} (corresponding to K_m in previous equations) and n is the Hill coefficient.

Downloaded from dmd.aspetjournals.org at ASPET Journals on April 9, 2024

DMD Fast Forward. Published on April 7, 2010 as DOI: 10.1124/dmd.109.031435
This article has not been copyedited and formatted. The final version may differ from this version.

LC-DAD-UV analyses.

A Shimadzu HPLC system (Shimadzu, Kyoto, Japan), consisting of two LC-10AD *Vp* module pumps, a SLC-10A *Vp* system controller, a SIL-10AD *Vp* autosampler and a DGU-14-A on-line degasser, was used for the analysis. All the chromatographic separations were performed on a *Phenomenex Synergi 4µm POLAR C18* (150 * 4.6 mm) as a stationary phase protected by a C18-Security Guard™ (Phenomenex, Torrance, CA). The SPD-M10Avp photodiode array detector was used to detect the analyte at 330 nm. A LCSolution 1.24 software was used to process the chromatograms. Aliquots (20 µL) of supernatants obtained from incubations were injected onto HPLC system and isocratically eluted with a mobile phase (flow rate 1.0 mL/min) constituted by A= water (0.5% formic acid)/ B= acetonitrile (0.5% formic acid) 60:40. The eluants were filtered through a 0.45 µm pore size PVDF membrane filter prior to use. All the analyses were carried out at room temperature.

Method validation.

The LC-DAD-UV method was validated, following the ICH guideline (ICH, 2005), with respect to analyte stability, selectivity, linearity, accuracy, precision, detection and quantification limits.

Stability.

The stability of **CA-4G** during sample preparation was assessed by treating 150 µL of a **CA-4G** solution (6.0 µg/mL; 50 mM TRIS·HCl, pH 7.4) as reported in the HLM incubation procedure. The supernatant was analyzed in triplicate immediately and after 1 hour: no significant difference was observed between peak area values.

Selectivity.

Method selectivity was assessed with respect to interference arising from biological matrices (i.e. human microsomes, UGT isoforms and added cofactors) and UGT inhibitors. In the first case, incubations were performed in the absence of **CA-4** using the same components as standard incubations; sample preparation and HPLC analysis were carried out as reported above. To evaluate

Downloaded from dmd.aspetjournals.org at ASPET Journals on April 9, 2024

DMD Fast Forward. Published on April 7, 2010 as DOI: 10.1124/dmd.109.031435
This article has not been copyedited and formatted. The final version may differ from this version.

the interference of UGT inhibitors and their putative glucuronides, incubations were performed as reported for **CA-4** and analyzed by HPLC to evaluate the presence of peaks with the same retention time as **CA-4G.** In both cases no interference was observed.

Linearity.

Linearity was evaluated at nine concentration levels (0.075-10 µg/mL) of **CA-4G**. These were injected in triplicate and the peak areas were plotted on an Excel® spreadsheet (Microsoft, Redmond, WA). The linear regression equation was generated at nine levels calibration by least squares treatment of the data ($y = 10057.4x+377.5$ $r^2 = 0.9999$).

Accuracy.

This was determined at two concentration levels (1.5 and 10 µg/mL) by application of the analytical procedure to recovery studies, where a known concentration of standard **CA-4G** is spiked in the matrix sample solution. The accuracy studies gave recovery values of 105 and 101% at concentrations of 1.5 and 10 µg/mL respectively thus demonstrating that the method was accurate within the desired range.

Precision.

Precision was evaluated at two concentration levels (1.5 and 10 µg/mL) in terms of instrumental and *intra-day* repeatability as well as *inter-day* reproducibility. The instrumental repeatability was assessed by analyzing the same solution six times. The *intra-day* repeatability was investigated using six separate sample solutions which were analyzed in triplicate. The *inter-day* reproducibility was checked on four different days, by preparing and analysing in triplicate four separate sample solutions. The calculated % RSD of *intra-day* repeatability and *inter-day* reproducibility were always ≤ 5.0%

Limit of detection (LOD) and quantification (LOQ).

The limit of detection, determined by injecting progressively low concentration solutions, was 0.025 µg/mL (signal-to-noise ratio: 3). The LOQ value was then calculated resulting in 0.075 µg/mL.

Downloaded from dmd.aspetjournals.org at ASPET Journals on April 9, 2024

DMD Fast Forward. Published on April 7, 2010 as DOI: 10.1124/dmd.109.031435
This article has not been copyedited and formatted. The final version may differ from this version.

RESULTS

We investigated the kinetics of combretastatin A-4 glucuronidation in pooled HLM as well as a panel of nine recombinant UGT Supersomes™. **CA-4**, incubated in the presence of UDP-glucuronic acid, gave the formation of **CA-4G** being its identity confirmed by comparison of the retention time and UV spectrum with those of an authentic standard (Aprile et al., 2009). The analyses of incubations were performed using a validated LC-UV method. Selectivity, linearity, accuracy, precision, detection and quantification limits were assessed to ensure the reliability of kinetic results.

Human liver microsome glucuronidation of CA-4.

Human liver microsomes incubated in the presence of **CA-4** (7.5-500 µM) generated a significant amount of **CA-4G** , sufficient to obtain the *substrate concentration-glucuronidation velocity* curves reported in Fig. 2 and the Eadie-Hofstee (EH) plots (Suppl. 1). The corresponding kinetic parameters were determined by fitting the data obtained from microsomal incubations to the equations *1-3* to obtain the correlation coefficients (R^2) value. The results of the kinetic analyses showed that **CA-4** glucuronidation in HLM fitted the substrate inhibition model (*eq. 2*) and V_{max}, K_m and the substrate inhibition constant (K_i) parameters were thus calculated (Table 1).

Recombinant UGT isoforms glucuronidation of CA-4.

Combretastatin A-4 glucuronidation by recombinant UGT Supersomes™ was investigated using a panel of nine recombinant UGT isozymes (1A1, 1A3, 1A4, 1A6, 1A9, 2B4, 2B7, 2B15 and 2B17). **CA-4** glucuronidation velocities were evaluated at three different substrate concentrations (50, 100 and 200 µM) and reported in Fig. 3. UGT1A9 and UGT1A6, exhibited the highest glucuronosyltransferase activity, their velocities (at 100 µM substrate concentration) being 11.8 and 3.3 nmol/min/mg protein respectively. On the contrary, UGT1A1, A3, 2B7 and 2B17 exhibited low

Downloaded from dmd.aspetjournals.org at ASPET Journals on April 9, 2024

DMD Fast Forward. Published on April 7, 2010 as DOI: 10.1124/dmd.109.031435
This article has not been copyedited and formatted. The final version may differ from this version.

glucuronosyltransferase activity (0.7, 0.7, 0.2 and 0.4 nmol/min/mg protein respectively). Finally, UGT1A4, 2B4 and 2B15 isoforms showed negligible glucuronosyltransferase activity (< 0.03 nmol/min/mg protein). The *substrate concentration-glucuronidation velocity* curves of recombinant UGTs were also obtained and are reported in Fig. 2, while the Eadie–Hofstee (EH) plots are available in Suppl. 1. The corresponding enzyme kinetic parameters expressed as mean ± S.E. are listed in table 1. As reported for microsomes assay, the best fit and kinetic profile of UGT glucuronidation assays was determined by fitting the data points to the equations *1-3*, and thus obtaining the R^2 coefficient value. The first observation was that the kinetic profiles diverge from one enzyme source to another. In the case of UGT1A3, 2B7, 2B15 and 2B17, the data points exhibited a substrate inhibition profile (*eq. 2*). Moreover, glucuronidation kinetic data for UGT1A1 and 1A6 best fitted the sigmoidal kinetic model, their Hill coefficients being n = 0.78 and 1.61 respectively, indicating negative cooperativity ($n < 0$) or homotropic positive cooperative reaction ($n > 0$) (*eq. 3*). In UGT1A9 glucuronidation assay the data points fitted the substrate inhibition equation well (*eq. 2*). The observed high rate of formation of **CA-4G** (V_{max} = 12.78 ± 0.29) and the low K_m (6.98 ± 0.65) denoted that UGT1A9 was primarily responsible for the in vitro glucuronidation of combretastatin A-4.

Chemical inhibition of CA-4 glucuronidation.

Phenylbutazone, propofol, trifluoroperazine and 1-naphthol, when added to the HLM incubation mixture had a relevant and concentration–dependent inhibitory effect. In particular, as shown in Fig. 4, phenylbutazone, at a concentration of 1 mM , decreased enzymatic activity by approximately 50%. Similarly, trifluoperazine (500 µM), propofol (1 mM), and 1-naphthol (500 µM) decreased microsomal activity by 12 %, 22 % and 10% respectively. In addition, we also observed the moderating inhibitory effect of silibinin on HLM glucuronidation activity; when this was added to the incubation mixture at a concentration of 100 µM , the microsomal residual activity was found to be approximately 75%. Finally, AZT did not show any inhibitory effect on HLM glucuronidation

Downloaded from dmd.aspetjournals.org at ASPET Journals on April 9, 2024

DMD Fast Forward. Published on April 7, 2010 as DOI: 10.1124/dmd.109.031435
This article has not been copyedited and formatted. The final version may differ from this version.

activity. The inhibitory effect of 1-naphthol and trifluoperazine was also tested on UGT1A9 and UGT1A6 combretastatin glucuronidation. As shown in Suppl. 2, trifluoperazine inhibited UGT1A9 and UGT1A6 glucuronidation activity to a similar extent as HLM whereas 1-naphthol only inhibited UGT1A9 similarly to HLM less affecting UGT1A6 activity. Finally, the inhibitory effects of combretastatin A-4 glucuronide per se on **CA-4** glucuronidation by HLM and UGT1A9 were also studied. The addition of **CA-4G** in **CA-4** glucuronidation assays did not affect the enzymatic activity as revealed by the ~ 100% residual activity (Suppl. 3).

Downloaded from dmd.aspetjournals.org at ASPET Journals on April 9, 2024

DMD Fast Forward. Published on April 7, 2010 as DOI: 10.1124/dmd.109.031435
This article has not been copyedited and formatted. The final version may differ from this version.

DISCUSSION

Combretastatin A-4 is a new promising anticancer drug at present undergoing clinical study (Banerjee et al., 2008). The formation of related glucuronide as the major **CA-4** metabolite was demonstrated (Aprile et al., 2009) in rat and human liver fractions as well as in vivo in rat. Several pharmacokinetic studies have shown that the **CA-4** phosphate prodrug is rapidly dephosphorylated into the systemic circulation with a very short plasma half-life, with **CA-4** and its glucuronide (**CA-4G**) displaying longer disposition profile (Dowlati et al., 2002; Rustin et al., 2003). The aim of this study was to identify and characterize the UGT isoforms involved in combretastatin glucuronidation by incubation in human liver microsomes and recombinant UGTs Supersomes™. Firstly, optimization of the incubation conditions, in terms of linearity of metabolite formation with increased microsomal protein and incubation time was carried out with HLM. Secondly, we examined the activity and kinetics in HLM and then in a panel of nine commercially available recombinant UGT microsomes from baculovirus–infected insect cells. Recombinant UGT1A9 isozyme was the main isoform catalyzing the glucuronidation of **CA-4** (Fig. 3), and the resulting data points fitted the substrate inhibition profile well (*eq. 2*). UGT1A6 was recognized as making an important contribution to **CA-4** glucuronidation. In this instance, the data points well fitted the sigmoidal kinetic model (Hill profile), (*eq. 3*) its Hill coefficient being $n > 1$ (Table 1): these features indicated that a positive cooperative reaction had occurred. UGT1A1, which produced a moderate glucuronidation activity, also shared the Hill profile, but the Hill coefficient $n < 1$ suggests a negative cooperative reaction. Finally, UGT1A3, 2B7 and 2B17 contributed little to the glucuronidation of **CA-4** whereas the UGT1A4, 2B4 and 2B15 contributes were negligible (Fig. 3). UGT1A3, 1A9, 2B7, 2B15 and 2B17 exhibited a substrate inhibition profile thus fitting the data points in *eq. 2* well. This atypical kinetic behavior has been described as a two-site model in which one binding site is productive, whereas the other one is inhibitory and operable at high substrate concentration, resulting in decreased velocity with increased concentration (Hunzler and Tracy, 2002). Alternatively, a more recent kinetic characterization of the UGT1A subfamily suggests that

Downloaded from dmd.aspetjournals.org at ASPET Journals on April 9, 2024

DMD Fast Forward. Published on April 7, 2010 as DOI: 10.1124/dmd.109.031435
This article has not been copyedited and formatted. The final version may differ from this version.

binding of the substrate to the enzyme-UDP complex leads to a nonproductive complex that slows the completion of the catalytic cycle. Furthermore *eq. 2* fits the inhibition data well when it was measured at only one UDPGA concentration. (Luukkanen et al., 2005). It is also worth mentioning (Hunzler and Tracy, 2002) that it is important to perform these studies having eliminated as far as possible any artifactual sources of atypical kinetics like significant substrate depletion or low substrate solubility. With the express purpose of eliminating these effects, incubations in the presence of HLM and recombinant UGT1A9 needed to be carried out using a low protein concentration (0.05 mg/mL) in order to avoid the total substrate depletion at a low substrate concentration. Moreover, we could not increase the substrate concentration to 500 µM as the low solubility of **CA-4** would have required the use of a high final acetonitrile concentration (> 1%) in the incubation buffer. The low protein concentration needed in HLM and recombinant UGT1A9 assay, suggests that they are characterized by high affinity for combretastatin A-4. It is known that the use of a multienzyme system like HLM may have an impact on the type of kinetic observed (Soars et al., 2003); however, the fact that the substrate inhibition profile was seen throughout the incubations with HLM and five different UGT isoforms indicates that the observed atypical kinetic is not an artifact. Experiments conducted to inhibit glucuronidation activity identified phenylbutazone, propofol and 1-naphtol (inhibitors of UGT1A, 1A9, and 1A6/1A9 respectively) as effective inhibitors in HLM combretastatin glucuronidation. The inhibition of **CA-4** glucuronidation by trifluoperazine was demonstrated to be due to lack of selectivity of this probe substrate toward UGT1A4. Fig. 4 and Suppl. 2 showed that trifluoperazine (> 100 µM) effectively inhibited UGT1A9 and UGT1A6 combretastatin glucuronidation to a similar extent as HLM. This data is consistent with the negligible UGT1A4 glucuronidation activity revealed in kinetic experiments. Silibinin is known to be a potent inhibitor of UGT1A1, although UGT1A6 and 1A9 were also inhibited (Sridar et al., 2004). The moderate capability of silibinin to inhibit **CA-4** glucuronidation in HLM (Fig. 4) is consistent with the moderate capability of recombinant UGT1A1 in **CA-4** glucuronidation. Finally, the lack of inhibitory potency of AZT on HLM

Downloaded from dmd.aspetjournals.org at ASPET Journals on April 9, 2024

DMD Fast Forward. Published on April 7, 2010 as DOI: 10.1124/dmd.109.031435
This article has not been copyedited and formatted. The final version may differ from this version.

catalyzed **CA-4** glucuronidation indicates only a marginal potential for UGT2B7 to contribute to **CA-4** glucuronidation. The increasing availability of "probes" substrate and inhibitors for the individual UGTs could enable reliable identification of the UGT(s) responsible for glucuronidation in human liver microsomes. However when HLM are used as an enzyme source for UGT inhibition studies, the results should be interpreted carefully. Recently, Fujiwara and co-workers (2008) emphasised that attention should be paid to the inhibitory effects of UDP on UDP-glucuronosyltranferase activity, which may cause erroneous evaluations in inhibition studies using HLM. In particular they found that the inhibition of UGT1A1 and 1A4 activities in human liver microsomes could be attributed to the inhibitory effect of the UDP produced by UGT1A6-catalyzed 1-naphthol glucuronidation. However, our observation of the prominent inhibition by 1-naphthol in HLM **- CA-4** glucuronidation could be attributed to the inhibition of UGT1A6 and UGT1A9 as the UGT1A1 and 1A4 role in **CA-4** glucuronidation was very moderate as displayed in recombinant isoforms glucuronidation assays.

In conclusion this investigation demonstrated that the glucuronidation, the main metabolic pathway of combretastatin A-4, was mainly catalyzed by UGT1A9 and UGT1A6 isoforms being its kinetic an atypical type.

Downloaded from dmd.aspetjournals.org at ASPET Journals on April 9, 2024

DMD Fast Forward. Published on April 7, 2010 as DOI: 10.1124/dmd.109.031435
This article has not been copyedited and formatted. The final version may differ from this version.

REFERENCES

Aprile S, Del Grosso E, Tron GC and Grosa G (2007) In vitro metabolism study of combretastatin A-4 in rat and human liver microsomes. *Drug Metab Dispos* **35:** 2252 – 2261.

Aprile S, Del Grosso E, and Grosa G (2009) In vitro and in vivo phase II metabolism of combretastatin A-4: evidence for the formation of a sulphate conjugate metabolite. *Xenobiotica* **39:** 148 – 161.

Banerjee S, Wang Z, Mohammad M, Sarkar FH and Mohammad RM (2008) Efficacy of selected natural products as therapeutic agents against cancer. *J Nat Prod* **71:** 492 – 496.

Brown RT, Fox BW, Hadfield JA, McGown AT, Mayalarp SP, Pettit GR and Woods JA (1995) Synthesis of water – soluble sugar derivatives of combretastatin A-4. *J Chem Soc, Perkin Trans 1* 577 – 581.

Dowlati A, Robertson K, Cooney M, Petros WP, Stratford M, Jesberger J, Rafie N, Overmoyer B, Makkar V, Stambler B, Taylor A, Waas J, Lewin JS, McCrae KR, Scot, Remick SC (2002) A phase I pharmacokinetic and translational study of the novel vascular targeting agent combretastatin A-4 phosphate on a single-dose intravenous schedule in patients with advanced cancer. *Cancer Res* **62:** 3408 – 3416.

Fujiwara R, Nakajima M, Yamanaka H, Katoh M, and Yokoi T (2008) Product inhibition of UDP-glucuronosyltransferase (UGT) enzymes by UDP obfuscates the inhibitory effects of UGT substrates. *Drug Metab Dispos* **36:** 361 – 367.

Houston JB and Kenworthy KE (2000) In vitro – in vivo scaling of CYP kinetic data not consistent with the classical Michaelis–Menten model. *Drug Metab. Dispos.* **28:** 246–254.

Hutzler JM and Tracy TS (2002) Atypical kinetic profiles in drug metabolism reactions. *Drug Metab Dispos* **30:** 355 – 362.

ICH-Harmonised Tripartite Guideline (2005) Validation of Analytical Procedures: Text and

Downloaded from dmd.aspetjournals.org at ASPET Journals on April 9, 2024

DMD Fast Forward. Published on April 7, 2010 as DOI: 10.1124/dmd.109.031435
This article has not been copyedited and formatted. The final version may differ from this version.

Methodology.

Izukawa T, Nakajima M, Fujiwara R, Yamanaka H, Fukami T, Takamiya M, Aoki Y, Ikushiro S, Sakaki T and Yokoi T (2009) Quantitative analysis of UGT1A and UGT2B expression levels in human livers. *Drug Metab Dispos* **37:** 1759 – 1768.

Luukkanen L, Taskinen J, Kurkela M, Kostiainen R, Hirvonen J and Finel M (2005) Kinetic characterization of the 1A subfamily of recombinant human UDP-glucuronosyltransferases. *Drug Metab Dispos* **33:** 1017 – 1026.

Kerdpin O, Knights KM, Elliot DJ and Miners JO (2008) In vitro characterization of human renal and hepatic frusemide glucuronidation and identification of the UDP-glucuronosyltranferase enzymes involved in this pathway. *Biochem Pharmacol* **76:** 249 – 257.

McGown AT and Fox BV (1989) Structural and biochemical comparison of the antimitotic agents colchicine, combretastatin-A4 and amphetinile. *Anti-Cancer Drug Des* **3:** 249 – 254.

Ohno S and Nakajin S (2009) Determination of mRNA expression of human UDP-glucuronosyltransferases and application for localization in various human tissues by real-time reverse transcriptase-polymerase chain reaction. *Drug Metab Dispos* **37:** 32 – 40 .

Pettit GR, Singh SB, Hamel E, Lin CM, Alberts DS and Garciakendall D (1989) Antineoplastic agent 145. Isolation and structure of the strong cell-growth and tubulin inhibitor combretastatin-A4. *Experientia* **45:** 209 – 211.

Picard N, Ratanasavanh D, Prémaud A, Le Meur Y, and Marquet P (2005) Identification of the UDP-glucuronosyltransferase isoforms involved in mycophenolic acid phase II metabolism. *Drug Metab Dispos* **33:** 139 – 146.

Rustin GJS, Galbraith SM, Anderson H, Stratford M, Folkes LK, Sena L, Gumbrell L, Price PM (2003) Phase I clinical trial of weakly combretastatin A4 phosphate: Clinical and pharmacokinetic results. *J Clin Oncol* **21:** 2815 – 282.

Soars MG, Ring BJ and Wrighton ST (2003) The effect of incubation conditions on the enzyme

Downloaded from dmd.aspetjournals.org at ASPET Journals on April 9, 2024

DMD Fast Forward. Published on April 7, 2010 as DOI: 10.1124/dmd.109.031435
This article has not been copyedited and formatted. The final version may differ from this version.

kinetics of UDP-glucuronosyltranferases. *Drug Metab Dispos* **31:** 762 – 767.

Sridar C, Goosen TC, Kent UM, Williams JA, and Hollenberg PF (2004) Silybin inactivates cytochromes P450 3A4 and 2C9 and inhibits major hepatic glucuronosyltransferases. *Drug Metab Dispos* **32:** 587 – 594.

Tozer GM, Kanthou C, and Baguley BC (2005) Disrupting tumor blood vessels. *Nat Rev Cancer* **5:** 423-435.

Uchaipichat V, Mackenzie PI, Elliot DJ, and Miners JO (2006) Selectivity of substrate (trifluoperazine) and inhibitor (amitriptyline, androsterone, canrenoic acid, hecogenin, phenylbutazone, quinidine, quinine, and sulfinpyrazone) "probes" for human UDP-glucuronosyltransferases. *Drug Metab Dispos* **34:** 449 – 456.

Downloaded from dmd.aspetjournals.org at ASPET Journals on April 9, 2024

DMD Fast Forward. Published on April 7, 2010 as DOI: 10.1124/dmd.109.031435
This article has not been copyedited and formatted. The final version may differ from this version.

FOOTNOTES

This work was supported by M.I.U.R.-PRIN 2007, Italy.

Downloaded from dmd.aspetjournals.org at ASPET Journals on April 9, 2024

DMD Fast Forward. Published on April 7, 2010 as DOI: 10.1124/dmd.109.031435
This article has not been copyedited and formatted. The final version may differ from this version.

LEGENDS FOR FIGURES

Fig. 1. Structures of combretastatin A-4 (**CA-4**) and its glucuronide metabolite (**CA-4G**).

Fig. 2. Enzyme kinetics of **CA-4** glucuronidation in HLM and recombinant human UGT isozymes. Data is reported as mean ± S.E., $n = 3$.

Fig. 3. Combretastatin A-4 glucuronidation activity of recombinant human UGT isozymes in microsomes from baculovirus-infected insect cells. Each bar represents the mean ± S.E. of triplicate determinations. The glucuronidation velocity is represented at three different **CA-4** concentrations (50, 100 and 200 µM).

Fig. 4. Effects of increased concentrations of phenylbutazone, silibinin, trifluoperazine, propofol, AZT and 1-naphthol in **CA-4G** formation in HLM. Each bar represents the mean ± S.E. of triplicate determinations.

Downloaded from dmd.aspetjournals.org at ASPET Journals on April 9, 2024

TABLES

Table 1. Kinetic parameters of **CA-4** glucuronidation in liver microsomes and UGT isoforms.

Protein Source	K_m	V_{max}	K_i	S_{50}	Hill coefficient *n*	Goodness of Fit (R^2)
HLM [a]	33.26 ± 2.90	41.98 ± 1.66	1126 ± 185.5	-	-	0.99
UGT1A1 [b]	-	2.20 ± 0.31	-	228.9 ± 88.5	0.78 ± 0.08	0.99
UGT1A3 [a]	46.48 ± 12.52	1.53 ± 0.23	295.0 ± 94.4	-	-	0.92
UGT1A4	N.D.	N.D.	N.D.	N.D.	N.D.	N.D.
UGT1A6 [b]	-	3.95 ± 0.13	-	44.80 ± 3.54	1.61 ± 0.16	0.98
UGT1A9 [a]	6.98 ± 0.65	12.78 ± 0.29	2271 ± 490.9	-	-	0.92
UGT2B4	N.D.	N.D.	N.D.	N.D.	N.D.	N.D.
UGT2B7 [a]	4.95 ± 0.64	0.236 ± 0.007	6761 ± 4541	-	-	0.90
UGT2B15 [a]	41.74 ± 12.37	0.067 ± 0.009	2182 ± 1900	-	-	0.91
UGT2B17 [a]	47.16 ± 12.34	0.70 ± 0.09	1756 ± 1166	-	-	0.93

[a] substrate inhibition model; *eq. 2.*
[b] sigmoidal kinetic model (Hill equation); *eq. 3.*
V_{max} (nmol/min/mg protein), K_m, K_i, S_{50} (μM).
N.D. not determined since activity below LOQ was observed.

Downloaded from dmd.aspetjournals.org at ASPET Journals on April 9, 2024

DMD Fast Forward. Published on April 7, 2010 as DOI: 10.1124/dmd.109.031435
This article has not been copyedited and formatted. The final version may differ from this version.

FIGURE 1

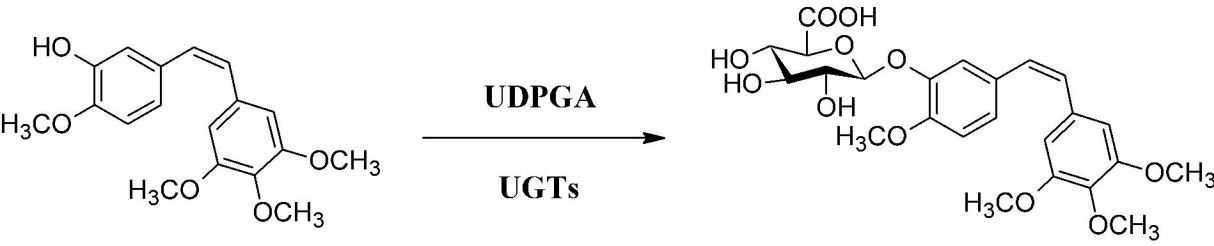

CA-4 **CA-4G**

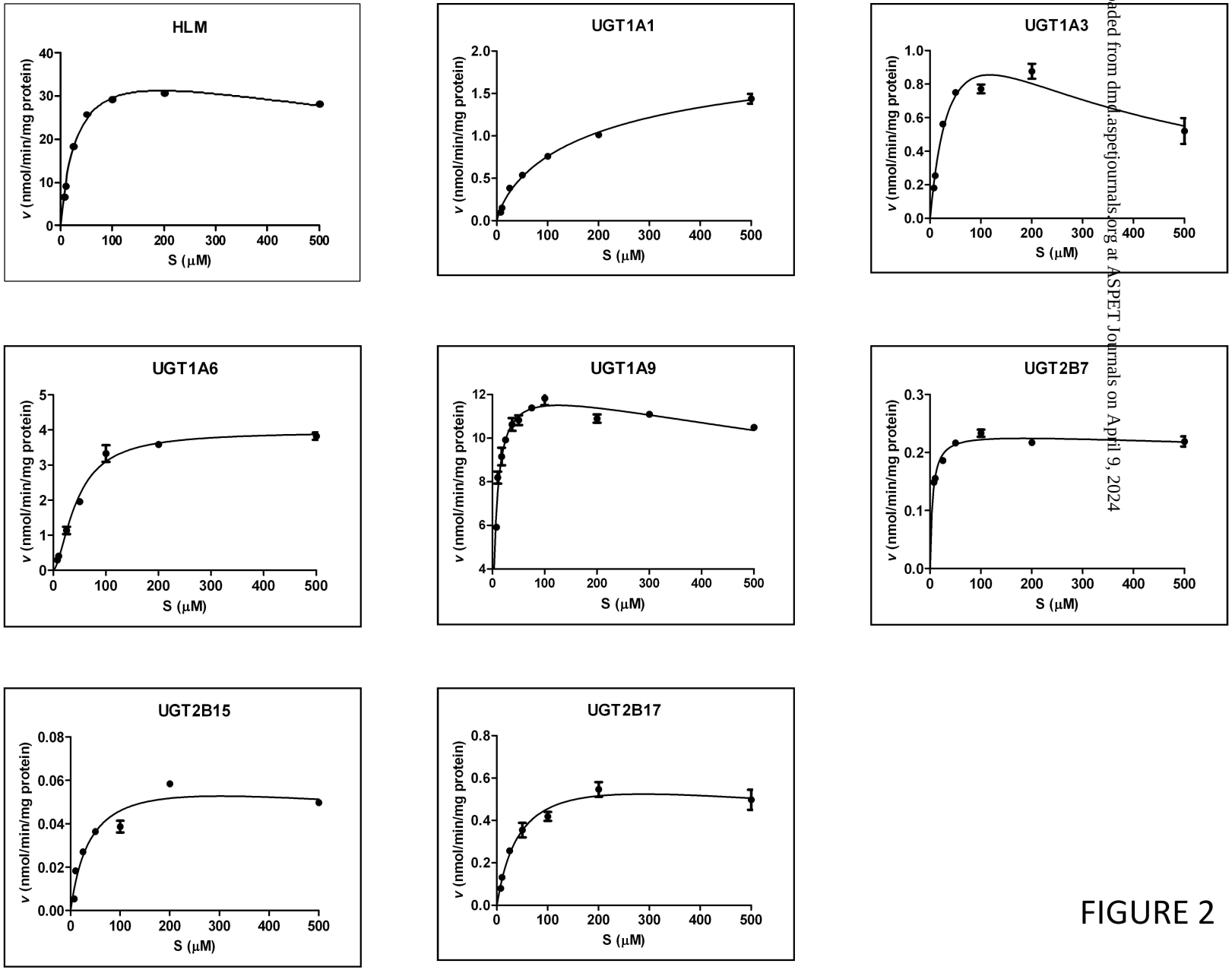

FIGURE 2

Downloaded from dmd.aspetjournals.org at ASPET Journals on April 9, 2024

FIGURE 3

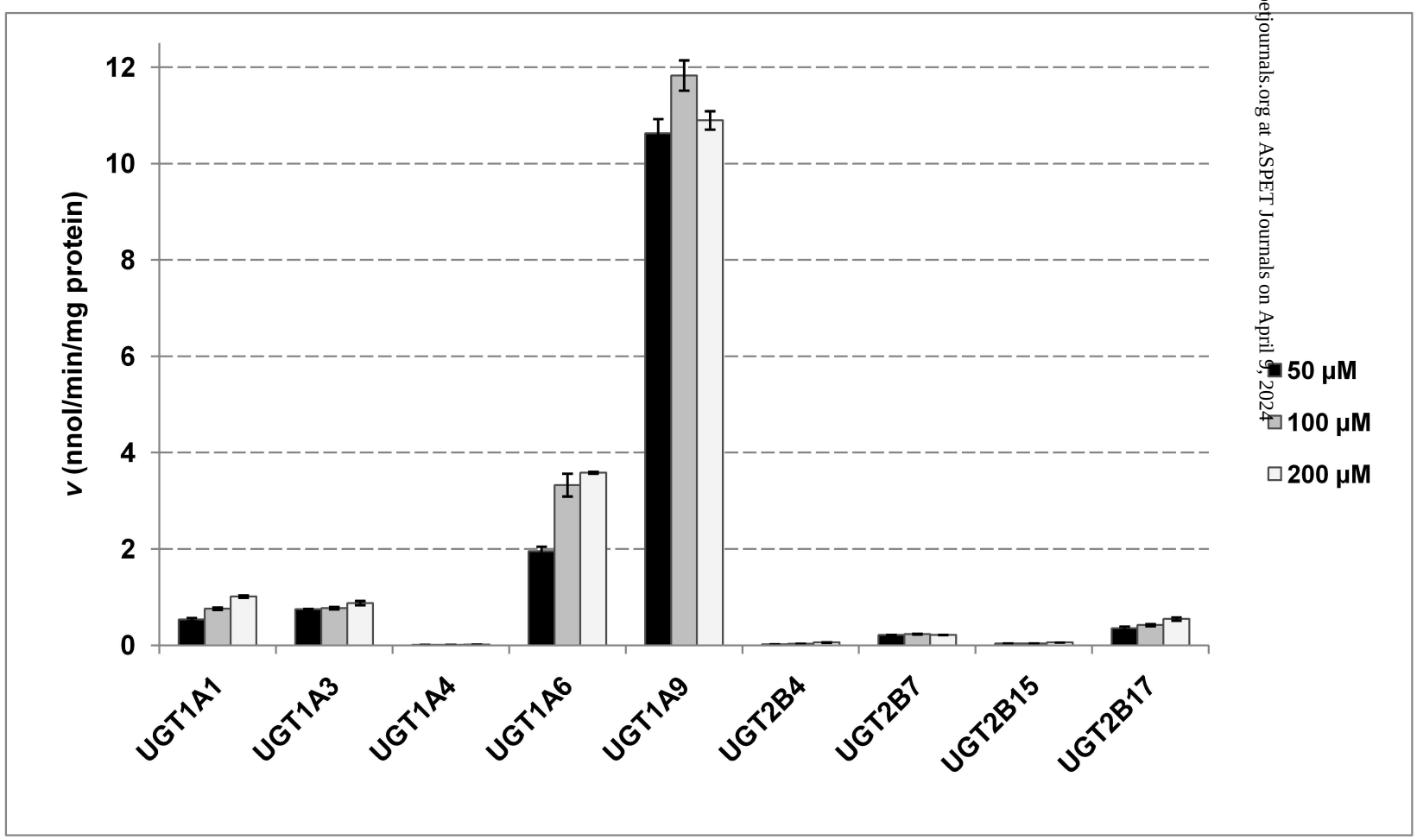

Downloaded from dmd.aspetjournals.org at ASPET Journals on April 9, 2024

FIGURE 4

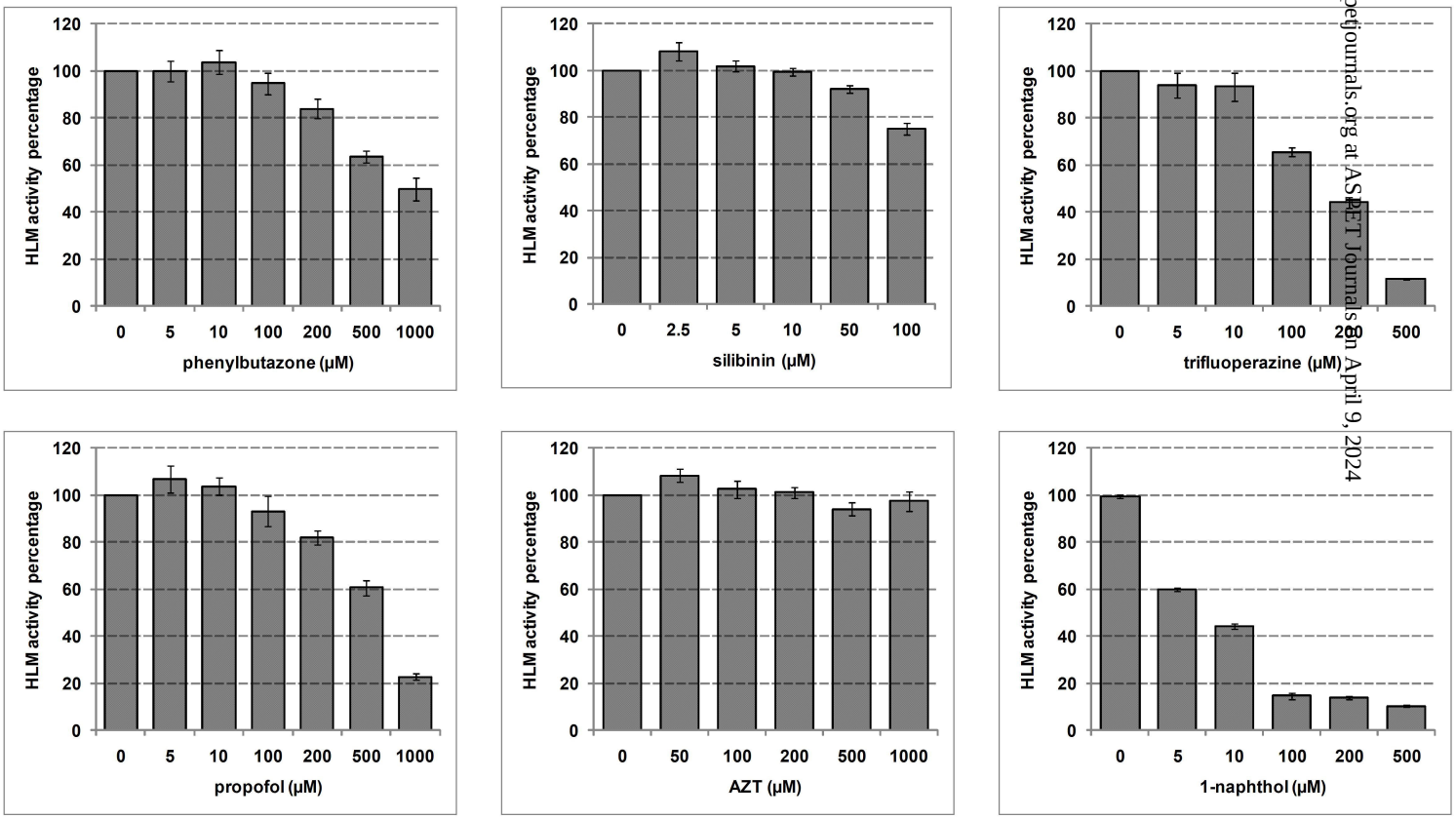

Downloaded from dmd.aspetjournals.org at ASPET Journals on April 9, 2024